Nonlithographic epitaxial Sn_xGe_{1-x} dense nanowire arrays grown on Ge(001)

Regina Ragan,[a] Channing C. Ahn, and Harry A. Atwater
Thomas J. Watson Laboratory of Applied Physics, California Institute of Technology, Pasadena, California 91125

(Received 26 March 2002; accepted 29 January 2003)

We have grown 1-μm-thick Sn_xGe_{1-x}/Ge(001) epitaxial films with $0<x<0.085$ by molecular-beam epitaxy. These films evolve during growth into a dense array of Sn_xGe_{1-x} nanowires oriented along [001], as confirmed by composition contrast observed in scanning transmission electron microscopy in planar view. The Sn-rich regions in these films dominate optical absorption at low energy; phase-separated Sn_xGe_{1-x} alloys have a lower-energy band gap than homogeneous alloys with the same average Sn composition. © *2003 American Institute of Physics.* [DOI: 10.1063/1.1563834]

Self-assembly as a means of nanostructures fabrication is receiving considerable attention for producing regular arrays of dots and wires with feature sizes on the order of 1–20 nm. A wide variety of methods are employed to fabricate self-assembled structures, such as DNA templating,[1] Langmuir–Blodgett molecular assembly,[2,3] and epitaxial growth. The latter is further developed than the former two methods. Epitaxial growth of quantum wires is achieved along step edges[4] and via phase separation.[5] Our investigation of phase-separated Sn_xGe_{1-x} alloys is also motivated by interest in Si-compatible optoelectronic materials.

Alloying Sn with Ge in a random solid solution induced an indirect-to-direct energy band-gap transition near a Sn composition of 10% for 100-nm-thick, coherently strained Sn_xGe_{1-x} films on Ge(001),[6] as well as for 300-nm-thick strain-relieved Sn_xGe_{1-x} films on Si(001).[7] These metastable films were grown by molecular-beam epitaxy (MBE). The details of the Sn_xGe_{1-x} growth were described elsewhere.[6] A dramatic change in morphology occurred during MBE growth of 1-μm-thick Sn_xGe_{1-x}/Ge(001) films under the same growth conditions. In this letter, microstructure analysis of 1-μm-thick Sn_xGe_{1-x}/Ge(001) films demonstrates that Sn segregated during growth to form Sn-rich Sn_xGe_{1-x} nanowire arrays oriented along [001] embedded in a Ge epitaxial film. The microstructure was characterized with transmission electron microscopy (TEM) and atomic force microscopy (AFM), and the average composition of the Sn_xGe_{1-x} nanowire arrays and the surrounding Ge matrix was determined by Rutherford backscattering spectroscopy. In addition, Fourier transform infrared (FTIR) transmittance measurements demonstrate a decrease in the direct energy band gap with phase separation, and indicate the onset of an indirect to direct band-gap transition at a lower average Sn composition than homogeneous alloys. Therefore, Sn phase separation can be exploited to obtain Sn_xGe_{1-x} nanowire arrays on Ge(001) having a direct energy band gap but a lower misfit than homogeneous Sn_xGe_{1-x}/Ge(001) films having the same *average* Sn composition.

Shown in Fig. 1(a) is a TEM two-beam image of a 1-μm-thick $Sn_{0.03}Ge_{0.97}$ film taken with $(\bar{2}\bar{2}0)$ diffraction planes excited ($\mathbf{g}=[\bar{2}\bar{2}0]$). This TEM image exhibits bands of contrast along [001]. The dark bands are measured as 23 nm in diameter with a period of 65 nm. The $Sn_{0.03}Ge_{0.97}$ film is single crystalline, as seen in the diffraction patterns along the [110] in Fig. 1(c), and [001] zone axes in Fig. 1(d). In Fig. 1(b), a two-beam TEM image with $\mathbf{g}=[004]$ exhibits significantly less contrast than the TEM image seen in Fig. 1(a). Contrast observed in conventional TEM images is due to both strain and composition. In kinematical theory for diffracted intensity under two-beam conditions,[8] strain contrast arises from an interaction between the lattice distortion ($\delta\mathbf{r}$) and the reciprocal lattice vector ($\mathbf{g}$) in the mathematical form of a dot product. If Sn segregates along the elastically soft (100) and (010) planes, then the larger Sn atoms coherently distort the lattice and $\delta\mathbf{r}=[100]$ and [010]. Since $\delta\mathbf{r}$ and $\mathbf{g}$ are orthogonal when $\mathbf{g}=[004]$, strain contrast is minimized and the remaining contrast is mainly compositional contrast. Hence, the decrease in contrast observed experi-

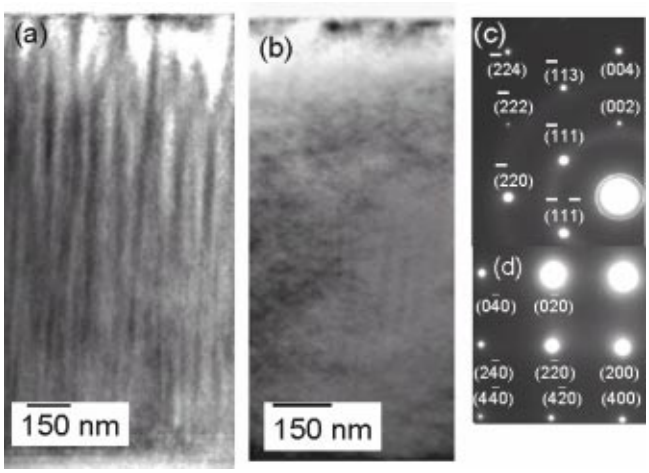

FIG. 1. Cross-sectional TEM analysis of 1-μm-thick $Sn_{0.03}Ge_{0.97}$ alloy imaged under two-beam conditions with (a) $\mathbf{g}=[\bar{2}\bar{2}0]$ and (b) $\mathbf{g}=[004]$. Diffraction patterns along (c) [110] and (d) [001] zone axes.

[a]Present address: Quantum Science Research, Hewlett-Packard Laboratories, 1501 Page Mill Road, Palo Alto, California 94304; electronic mail: Regina_Ragan@hp.com

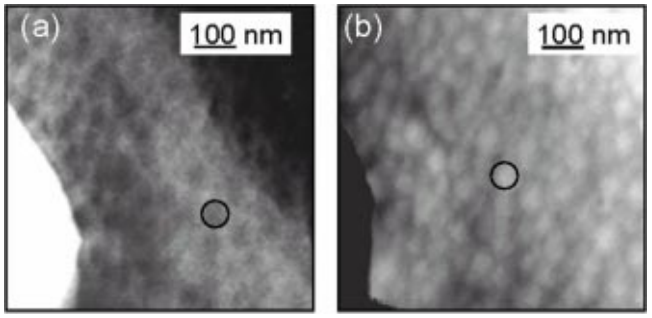

FIG. 2. Planar view STEM images of 1-μm-thick $Sn_{0.03}Ge_{0.97}$ alloy taken under (a) bright-field and (b) dark-field conditions. The Sn-rich nanowires are seen as dark circular regions in (a) and bright circular regions in (b) when observed in planar view. The same feature in both images is circled.

mentally under $\mathbf{g}=[004]$ two-beam conditions indicates Sn phase separation along (100) and (010) planes.

In order to prove Sn phase separation, the technique of Z-contrast imaging[9] was employed using scanning TEM (STEM) in planar view with a spot size of 5 nm. The bright-field image was taken with electrons having scattering angles <80 mrad. It includes diffracted and transmitted beams yielding both strain and composition contrast in the image. During dark-field imaging, an annular detector was placed to allow only elastically scattered electrons with scattering angles >80 mrad to contribute to the image. The contrast observed in dark-field images is mainly due to composition because diffraction intensity is attenuated at wide scattering angles.[9] A bright-field STEM image, shown in Fig. 2(a), has dark circular regions with approximately the same periodicity, 70 nm, observed in cross-sectional TEM [Fig. 1(a)]. In the dark-field STEM image, seen in Fig. 2(b), Sn phase separation is evident as Sn-rich regions appear as bright circular regions. The higher electron intensity in Fig. 2(b) is due to the higher cross section of Sn versus Ge for elastically scattered electrons. The interface between the Sn-rich and Ge-rich regions does not appear to be abrupt.

A periodic surface undulation with feature heights on the order of 1–2 nm was measured in AFM and was found to be well correlated to the periodicity (λ) of the Sn_xGe_{1-x} nanowire arrays observed in TEM. An AFM image of a $Sn_{0.018}Ge_{0.982}$ film is shown in Fig. 3(a). The autocorrelation function $G(k)$ of the topographical AFM image, plotted as asterisks in Fig. 3(b), was calculated to determine the dominant wave vector ($k=2\pi/\lambda$) of the nanowire arrays that is exhibited as the maxima of $G(k)$. In order to establish that the periodic surface undulation was not due to stochastic roughening as a result of the low growth temperature, but rather to strain and composition effects, a curve for unstrained Ge/Ge(001) grown at the same growth temperature ($T=433$ K) was plotted as open squares in Fig. 3(b). $G(k)$ for this unstrained Ge film did not have a maxima, as is typical for a stochastically roughened surface, and the peak decayed as k^{-2}.[10] $G(k)$ provides additional information; the power dependence of the wave vector as $G(k)$ decays is the signature of the physical mechanism dominating surface smoothing. $G(k)$ for the strained Sn_xGe_{1-x} films decayed as k^{-3}. A decay of k^{-3} of $G(k)$ and the absence of Sn phase separation for thinner films is agreement with a linear instability model for phase separation during dynamic growth.[11]

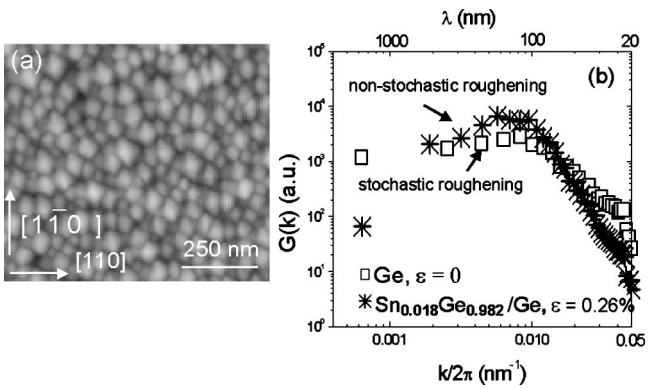

FIG. 3. (a) Planar view AFM image of Sn_xGe_{1-x}/Ge with $x=0.018$, $\varepsilon=0.26\%$. (b) autocorrelation function $G(k)$, vs wave vector with $T=433$ K: Ge (open squares) and Sn_xGe_{1-x}/Ge, $x=0.018$ (asterisks).

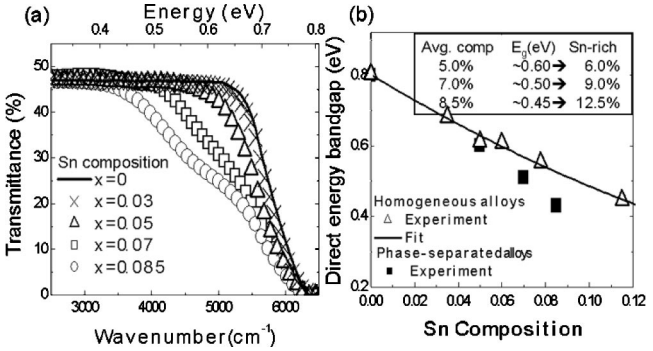

FIG. 4. (a) FTIR transmittance vs wave number for 1-μm-thick Sn_xGe_{1-x} alloys with $0<x<0.085$. (b) Energy band gap vs Sn composition for 1-μm-thick, phase-separated Sn_xGe_{1-x} alloys (closed squares) and 0.1-μm-thick homogeneous alloys (open triangles). Inset estimates the Sn composition in the Sn-rich regions from the band gap energy.

It is well known that a film in compression, as is Sn_xGe_{1-x}/Ge(001), can relieve coherency energy without dislocation introduction by forming a surface undulation with a larger lattice parameter at the crest of the undulation.[12,13] During dynamic growth, Sn, the larger atom, may segregate to regions with the larger lattice parameter via surface diffusion. In turn, these compositional fluctuations across the surface of the film introduce additional strain fields that amplify the driving force for Sn phase separation.[11,14] STEM images confirm Sn phase separation and TEM two-beam images give evidence of Sn segregation along elastically soft (100) and (010) planes. In addition, the decay of k^{-3} of $G(k)$ portends Sn phase separation during dynamic growth. The effect of strain and composition on the experimentally measured periodicity of Sn_xGe_{1-x} nanowire arrays was compared to that predicted by a linear instability model and shows good agreement.[15]

FTIR transmittance of Sn_xGe_{1-x}/Ge(001) nanowire arrays was performed between 2000 and 8000 cm^{-1}, shown in Fig. 4(a). Visual analysis of Fig. 4(a) reveals that the absorption edge shifts to lower energies with increasing Sn composition and the $Sn_{0.07}Ge_{0.93}$ alloy exhibits a sharper absorption edge, indicative of a direct energy band-gap material, than the $Sn_{0.05}Ge_{0.95}$ alloy. In agreement with previous measurements of homogeneous Sn_xGe_{1-x} alloys,[6,7] the direct energy band gap decreases with increasing Sn composition. In con-

trast to previous measurement, the indirect to direct band-gap transition appears to occur in phase-separated alloys at an average Sn composition of $x<0.07$, compared to $x<0.10$ for homogeneous alloys. For $x=0.085$, the transmittance curve appears to have two distinct points for the onset of absorption. Previous measurements of homogeneous Sn_xGe_{1-x} alloys demonstrated that the energy band gap varies with Sn composition; therefore, the observation of multiple points for the onset of absorption is attributed to a distribution of Sn compositions in the film resulting from the lack of an abrupt interface between the Sn-rich and the Ge-rich regions. An estimate of the direct energy band gap of phase-separated Sn_xGe_{1-x} films with Sn composition between $0<x<0.085$ was determined by modeling the absorption edge of the transmittance spectra with a power law dependence of the band-gap energy.[6,16] The lowest value of the direct energy band gap of phase-separated alloys, plotted as squares in Fig. 4(b), was lower than homogeneous alloys having the same average Sn composition. Since the Sn-rich regions appear to dominate absorption near the absorption edge, the peak Sn composition in the phase-separated films was extrapolated by comparing the measured value of the energy band gap of phase-separated alloys with that of homogeneous alloys.[6] The value of the peak Sn composition in the nanowires is shown in the inset of Fig. 4(b).

We have grown 1-μm-thick Sn_xGe_{1-x} nanowire arrays oriented along [001] on Ge(001). Sn phase separation was evident in TEM and STEM. The onset of absorption in FTIR transmittance measurements indicated a decrease in the energy band gap as well as a direct energy band gap at lower *average* Sn compositions with Sn phase separation in comparison to homogeneous Sn_xGe_{1-x}/Ge(001) alloys.

The National Science Foundation supported this work. One author (R. R.) acknowledges support in the form of an Intel fellowship.

[1] J. K. N. Mbindyo, B. D. Reiss, B. R. Martin, C. D. Keating, M. J. Natan, and T. E. Mallouk, Adv. Mater. **13**, 249 (2001).
[2] C. D. Bain and G. M. Whitesides, Angew. Chem. **101**, 522 (1989).
[3] A. Ulman, *Introduction to Thin Organic Films: From Langmuir-Blodgett to Self-Assembly* (Academic, Boston, 1991).
[4] H. Sunamura, N. Usami, Y. Shiraki, and S. Fukatsu, Appl. Phys. Lett. **68**, 1847 (1996).
[5] R. D. Twesten, D. M. Follstaedt, S. R. Lee, E. D. Jones, J. L. Reno, J. Mirecki Millunchick, A. G. Norman, S. P. Ahrenkiel, and M. A. Mascarenhas, Phys. Rev. B **60**, 13619 (1991).
[6] R. Ragan and H. A. Atwater, Appl. Phys. Lett. **77**, 3418 (2000).
[7] G. He and H. A. Atwater, Phys. Rev. Lett. **79**, 1937 (1997).
[8] B. J. Fultz and J. Howe, *Transmission Electron Microscopy and Diffractometry of Materials* (Springer, Pasadena, 2000).
[9] S. J. Pennycook, S. D. Berger, and R. J. Culbertson, J. Microsc. **144**, 229 (1986).
[10] W. M. Tong and R. S. Williams, Annu. Rev. Phys. Chem. **45**, 401 (1994).
[11] J. E. Guyer, S. A. Barnett, and P. W. Voorhees, J. Cryst. Growth **217**, 1 (2000).
[12] R. J. Asaro and W. A. Tiller, Metall. Trans. **3**, 1789 (1972).
[13] M. A. Grinfel'd, Sov. Phys. Dokl. **290**, 1358 (1986).
[14] F. Glas, Phys. Rev. B **55**, 11277 (1997).
[15] R. Ragan, J. E. Guyer, and H. A. Atwater (unpublished).
[16] J. I. Pankove, *Optical Processes in Semiconductors* (Dover, New York, 1975).